atom. Here we have all eight nearest neighbors displaced by roughly this amount, and their perturbations add at the unit cell containing the quadrupole moment under consideration, so we guess ϕ_0 is 10 eV or less.

Combining all the relations above we get

$$V_s'/V_s = 3\phi_0\lambda/a_0^2 M\omega_D^2\langle r^{-3}\rangle_d a_0^3 = 3\phi_0\lambda/Mc_s^2 a_0^3\langle r^{-3}\rangle_d.$$

Using the guesses for $\langle r^{-3}\rangle_d$, λ, and ϕ_0 given above, this ratio is about 1/50, showing that the enhancement may conceivably be a few percent but that it is unlikely to make electric relaxation competitive with orbital relaxation. That would require that the ratio V_s'/V_s be about 50, and that either λ or ϕ_d be very much larger than estimated.

PHYSICAL REVIEW VOLUME 162, NUMBER 2 10 OCTOBER 1967

Local-Field Mapping in Mixed-State Superconducting Vanadium by Nuclear Magnetic Resonance

ALFRED G. REDFIELD
IBM Watson Laboratory, Columbia University, New York, New York

(Received 19 May 1967)

A 10-kG field was applied to polarize the spins; it was then quickly reduced below H_{c2}, and remained there for about 0.1 sec, during which time a transverse ac probe field of frequency ν_p was applied. Then the large dc field was reapplied and a rapid-passage resonance signal observed in order to measure the effect of the probe field, the decrease in this subsequent signal reflecting the NMR absorption. Except near H_{c2} the probe field only burns a small hole in the nuclear magnetization, and it was also necessary to move the vortex structure about by applying a 100-Hz field of a few gauss during the time that the sample was in the mixed state. Detailed studies are reported for a multiple foil sample of vanadium with main field perpendicular to the surface; aluminum foil was interleaved, and the flux density B was measured using the Al^{27} NMR by exactly the same field-cycling resonance as applied to the vanadium. The magnetization was measured ballistically in the same magnet and field cycle. For flux density around $\frac{1}{2}H_{c2}$ the line shape almost uniquely implies a triangular vortex lattice. At high probe power, the effect of the probe field is still confined to the same definite frequency range as at low power, as would be the case for a completely ordered vortex lattice; this implies order over several vortex-lattice spacings. Accurate measurements are presented of the field at a vortex center and at the saddle point halfway between two vortices, and of the average flux density B, as a function of H, in a fairly clean sample at 1.4°K. These parameters determine an accurate field map. Near H_{c2} the field at a vortex center equals H, with a deviation of second (or greater) order in $H-H_{c2}$. The linewidth is greater, for a given magnetization, than would be expected from solutions of the Ginsburg-Landau equations. By extrapolation to zero B, it is concluded that the field at the center of a vortex is 1.2 ± 0.2 times H_{c1}. The data are consistent, at low B, with a superposition model of independent vortices.

I. INTRODUCTION

CONVENTIONAL nuclear resonance studies of the field distribution in type-II superconductors are difficult because of the large resonance linewidths, baseline shift, and noise due to vortex motion, and sample inhomogeneity. Nevertheless, Gossard *et al.*[1] observed a structureless broadening in the NMR of vanadium in V_3Si and V_3Ga and Delrieux and Winter[2] succeeded in observing NMR directly in niobium close to H_{c2}. Much the same kind of information can be obtained using angular correlations.[3]

We have avoided these problems by using field cycling resonance.[4,5] This yields exactly the same information as conventional NMR but has the advantage that the signal can be observed in the normal state with less noise and baseline drift. The cycle is the same as that of Fig. 1 of the previous article,[6] except that τ was fixed at about 0.1 sec, and during that time a transverse rf field $H_p\cos 2\pi\nu_p t$ (which we will call the probe field) was applied perpendicular to the main field H_e.[7]

Typical subsequent signals are shown in Fig. 1, as a function of the probe frequency ν_p. Consider first the case where H_e is greater than H_{c2} (upper right hand points in Fig. 1), so that all but a negligible surface sheath is normal, and the local field inside the sample is everywhere uniform and equal to H_e. The probe field

[1] P. Pincus, A. C. Gossard, V. Jaccarino, and J. H. Wernick, Phys. Letters **13**, 21 (1964).
[2] J. M. Delrieux and J. M. Winter, Solid State Commun. **4**, 545 (1966).
[3] J. Alonso, Bull. Am. Phys. Soc. **12**, 519 (1967).
[4] N. F. Ramsey and R. V. Pound, Phys. Rev. **81**, 278 (1951).
[5] A. G. Redfield, Phys. Rev. **130**, 589 (1963).
[6] W. Fite, II, and A. C. Redfield, Phys. Rev. (preceding article), **162**, 358 (1967), to which the reader is referred for many experimental details and references not included in this article.
[7] The probe field was applied by switching the transmitter coil with a mercury relay to the amplifier described in Ref. 5. The input to this amplifier, normally grounded, was simultaneously switched to a signal generator, which was varied manually. Only a single frequency ν_p was used, unlike Ref. 5.

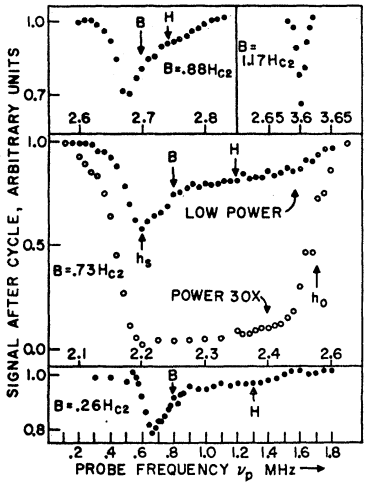

FIG. 1. Raw line-shape data at various fields and power levels.

has no effect until the nuclear resonance condition $2\pi\nu_p=\gamma H_e$ is approached.[8] Then, the probe field induces transitions between nuclear spin levels, with equal probability in both directions, and energy is absorbed by the spin system tending to destroy its magnetization and to reduce the subsequent signal. Thus, there is a sharp dip in the subsequent signal at the resonance condition (Fig. 1, upper-right-hand data).

If H_e is decreased below H_{c2}, there is, of course, a corresponding decrease in the frequency at which resonance is observed, but more important there is a broadening of the range over which resonance is observed (Fig. 1), as expected in the mixed state. We will discuss the significance of the line features in the mixed state in the next section.

This research started as a casual study in the normal state, above T_c, with $H_e=0$, to determine the order of magnitude of quadrupolar interactions in our sample.[5] In sample A we found that, for $H_e=0$, there was an apparently featureless absorption up to about 100 kc/sec, supporting the conclusions of the previous paper[6] about the magnitude of the quadrupolar interaction for a typical spin. (Such an interaction produces negligible second-order broadening of the $m_I=\frac{1}{2}\rightarrow-\frac{1}{2}$ transitions which is observed here, except perhaps at the lowest fields used.)

When we lowered the temperature below T_c, and raised H_e (with no added 100-Hz audio field), we were pleasantly surprised to find large signal variations within well-defined frequency ranges, as in Fig. 1. There are two reasons why the signal variations might be expected to be smaller than we observed: the lines are broad compared to those in the normal state; and also there is evidence[9] that the vortex structure is pinned against small external variations, so that relatively small variations in B (from the probe field, at frequency ν_p) might be diamagnetically shielded by a surface current.

The large linewidth should lead to the following difficulty: If the vortices are pinned, then each spin stays at some constant (in time) local field h, and precesses at some constant frequency $\gamma h/2\pi$ during the time τ. Although h is constant, it is different for different spins, the range of h being typically several hundred gauss. If a given spin is not at a point where h is within about 10 G of the resonance condition, it will not be much affected by the probe field, which will "burn a hole" in the line only near resonance. Thus the signal variation would be at most only about 10% for a 200-G linewidth, smaller than the nearly 100% effect observed.

At first we thought the large effect was evidence for slow diffusion of vortices during the 0.1 sec that ν_p is applied. This proved to be false, and the argument of the preceding paragraph does apply; the vortices are pinned. The reason for the large effect was that the initial runs were made with an improvised power-supply modification such that the field H_e was not regulated and the field actually decayed toward H_e with a time constant of some tens of milliseconds, during τ. In the hope of improving the resolution, the power supply was improved so that H_e was regulated and the cycle was really as shown in Fig. 1 of the previous article. The result of this improvement was that, except near H_{c2}, the effect of the probe field nearly disappeared. We then realized that the earlier small variation in H_e with the improvised supply produced a similar variation in B, which means a variation in vortex density (number per cm^2). Thus, since vortex quantization prohibits creation of a vortex inside the material, the vortex structure must have been slowly expanding itself as B decreased, so that vortices were moving away from the center. On realizing this, we partially removed the perfection of the regulation by applying a 100-Hz field of a few gauss magnitude, to move the vortex structure as described in the previous article, and the large effect returned. The 100-Hz field was used afterwards on all runs where the linewidth was more than 50 G.

As for the second question, the penetration of small ac fields into the sample, we can only say that they do apparently penetrate our samples to a distance comparable to the normal-state skin depth at 6 mc/sec. Perhaps it is easy for a transverse field to penetrate since this requires only an elastic bending of the vortices near the surface, not a change in the number threading

[8] Where throughout this article γ is the gyromagnetic ratio corrected for the 0.55% Knight shift ($\gamma/2\pi=1.125$ KHz/G for vanadium). Except close to H_{c2} the resolution of this experiment was not sufficient to study shifts in the Knight shift; at H_{c2}, no resolvable discontinuity in the Knight shift was found. Throughout this article, local fields are obtained from frequencies of line features using the Knight shifted γ.

[9] See, for example, B. Bertman and M. Strongin, Phys. Rev. **147**, 268 (1966), and references therein.

the sample. The 100-Hz field presents more of a problem[9]; perhaps it is easier for such a field to penetrate a flat stab than a longitudinal cylinder. It would be interesting to study these effects, systematically correlating NMR measurements with ac and dc susceptibility, but here we concentrated on local field measurement.

With reference to rf field penetration in the mixed state, there is one point which the reader should remember to avoid over-interpretation of the data. The rf field actually appears to be magnified inside the superconductor compared to the normal state. In Fig. 1, the same order of magnitude of probe field was used in all runs. Normally a greater rf field is needed to produce a given energy absorption for a wide line than for a narrow line. In the present case, with all its unusual features, we do not know how to prove that this is still true, but it seems plausible and, if true, indicates an rf field enhancement. A novel feature of this experiment is that the rf field will produce a tilting of the vortex structure which implies that near the surface, at least, there is also appreciable translation of the vortex lattice (at ν_p) and thus a strong rf field in the local field direction ($\cong$direction of H_e), proportional to the transverse gradient of local field. This rf field is along the axis of nuclear spin quantization and is therefore in just the wrong direction to induce transitions. However, it could do so because of state mixing produced by the residual quadrupole interaction; and it is also conceivable that there is a large transverse field resulting from pinning and/or bowing out of the vortex lines. The important thing is that this enhancement may be a function of position (of the vortex structure relative to a spin) so that the change in signal may not truly represent the line shape that would be observed with the same field without the enhancement. Thus, the line shape cannot be used to measure the second derivative of local field at a vortex, for example. However, unless the enhancement is strongly varying, the prominent bumps in the observed line shape are not likely to be shifted.

II. THE ABRIKSOV LATTICE

At this writing, the most direct evidence for the vortex lattice predicted by Abrikosov[10] is the neutron-diffraction experiment of Cribier *et al.*[11,12] From variations in scattering intensity for different runs on niobium, it is concluded that the "vortex crystallite" size is about 100 intervortex spacings, and from the position of the first Bragg peak and also the lack of a second peak it is concluded that the lattice must be triangular.

All our runs on samples A and B (except very close to H_{c2} or at very low field) show a dip at the low-field end corresponding to an increase in the energy absorption and presumably an increased number of spins at the corresponding field. The same has been observed in niobium by Delrieux and Winter.[2] This line shape does not tell us anything about long-range order, but it rules out many possible structures: square lattice, honeycomb lattice, laminar model, completely random, triangular lattice with very many imperfections.

The first calculation of the NMR line shape for a fluxoid lattice was that of Schmidt,[13] for the square lattice. His calculation, which was a coarse-grained integration of Abrikosov's square-lattice solution of the Ginsburg–Landau equations, showed a strong bump at a point about one third of the way from the minimum field limit of the line to the maximum. Our preliminary data appeared to conflict with his calculation, and it was clear from looking at the order parameter map[10] (which is identical to the field map) that the peak in the line corresponds to the saddle point in the field map, that is, to the field at a point halfway between two vortices. This is a two-dimensional version of a Van Hove singularity in the spectrum of lattice vibrations, and the singularity is logarithmic; the reader can convince himself that there is a singularity, or at least a great many spins located at that field, by looking at a field or order parameter map.

The corresponding singularity for the triangular lattice[14] is only 7% of the way from the low-field to the high-field end of the line, in the Abrikosov limit, in excellent agreement with our data. Lasher[15] kindly calculated the line shape for the triangular lattice, and also recalculated the square lattice; the two shapes are shown in Fig. 2. This difference between the expectation for the position of the singularity for the square and triangular lattice is not a quirk of the Abrikosov theory; it is a general result of geometry plus the assumption that field and current cannot vary by much over a coherence length.[15,16] For the square lattice, the saddle point in real space is equidistant from the nearest vortex and the nearest minimum point. For the triangular lattice, in real space, the saddle-vortex distance (S-V in Fig. 2) is $\sqrt{3}$ times greater than the saddle-minimum distance (S-M). Thus the saddle-point field tends also to be closer to the minimum field, an

[10] A. A. Abrikosov, Zh. Eksperim. i Teor. Fiz. **32**, 1442 (1957) [English transl.: Soviet Phys.—JETP **5**, 1174 (1957)].

[11] J. D. Cribier, B. Jacrot, L. Madhav Rao, and B. Farnoux, *Progress in Low Temperature Physics*, edited by C. J. Gorter (North-Holland Publishing Company, Amsterdam, 1967), Vol. V.

[12] See, however, a note added in proof by H. Trauble and U. Essman, Phys. Status Solidi **20**, 95 (1967); and Phys. Letters **24A**, 526 (1967).

[13] V. V. Shmidt, Zh. Eksperim. i Teor. Fiz. **46**, 649 (1964) [English transl.: Soviet Phys.—JETP **19**, 440 (1964)].

[14] W. H. Kleiner, L. M. Roth, and S. H. Autler, Phys. Rev. **133**, A1226 (1964), referred to as KRA in the text.

[15] W. Fite, II, and A. G. Redfield, Phys. Rev. Letters **17**, 381 (1966).

[16] W. Fite, II, and A. G. Redfield, Proceedings of the Tenth International Conference on Low Temperature Physics, Moscow, 1966 (to be published).

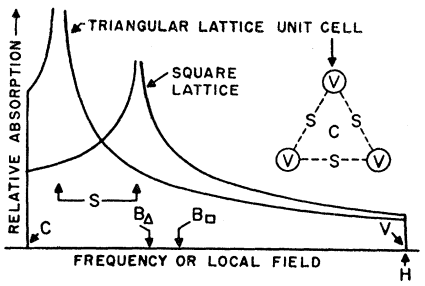

FIG. 2. Theoretical resonance line shapes calculated by Lasher on the basis of solutions to the Ginsburg-Landau equations in the Abrikosov limit. The horizontal scales are renormalized to give the same linewidth; in fact for a given material the square lattice width would be somewhat greater. The square ends of the lines are a consequence of the zero gradient of the field at the vortex center and the minimum point. The inset shows a unit cell of the vortex lattice, showing points of maximum field (V), minimum field (C), and the saddle point (S).

effect which is much greater than the real-space distance ratio suggests, because the field and current must be smoothly varying in space.

Practically the same predicted position for the singularity comes from the simplest artificial field distribution obtained by summing three $\cos(\mathbf{k}_i\cdot\mathbf{r})$ terms, with the three k_i's equal in magnitude and 120° apart in direction. Such a distribution is in better agreement with the neutron-diffraction data[11] (lack of a second-order Bragg peak) than is the corresponding solution of the Ginsburg-Landau equations. The same kind of cosine sum with square symmetry has its singularity exactly in the middle, of course.

Figure 3(a) may help convince the reader that the short-range order is triangular. We convoluted the theoretical line shapes of Fig. 2 with a Gaussian function, to smear out the line shapes by about 10%, to agree with the width of the end of the line at high field, and normalized the total linewidth and height to get good agreement with experiment for the triangular lattice. The experimental points are proportional to $-\ln\{[S(H_p)-S(\infty)]/[S(0)-S(\infty)]\}$, where $S(H_p)$ is the signal observed when the probe field equals H_p, $S(0)$ is that with no probe field, and $S(\infty)$ is the signal at very high probe power, which is mostly due to repolarization of the spin system during the time the field is turned on, just before observation at 6 kG. If one makes a simple spin-temperature assumption about the rate of energy absorption, then one concludes that this transformation of the data should give the absorption line shape which would be observed in conventional NMR. The excellent agreement between these points and the triangular line shape should not be taken too seriously since there were three parameters varied to fit the data (width, height, smearing), but it would not be possible to change these parameters to get nearly as good agreement with the square lattice curve. Closer to H_{c2} [Fig. 3(b)] it would be harder to make this distinction. For very low B, on the other hand, one has essentially an array of nearly isolated vortices, and the peak is expected to move toward the lower end of the line for any arrangement.

The honeycomb lattice would have a singularity close to the maximum field; the laminar model would have peaks at both ends, at least for long coherence length; any other lattice would have two or more singularities. A completely random distribution would have no singularities.

Fairly stringent, if difficult to define, limits are placed by our data on possible imperfection of the lattice, for B in the range around $\frac{1}{2}H_{c2}$. Here the ends of the line are well defined, although the lower end can never be resolved from the singularity. The power can be increased 10 to 100 times the level needed to get a 50% decrease in subsequent signal (points marked "high power" in Fig. 3). This washes out the structure within the line, but the ends of the line remain extremely sharp and unmoved, and there is no precursor absorption beyond the ends of the lines. Imperfections in the vortex lattice would lead to field excursions outside the perfect-lattice limits. These imperfections would be moved about by the 100-Hz audio field and lead to precursors of absorption at high power. Let us guess that our data show that fewer than 20% of the spins at minimum field points experience shifts in their resonance frequencies greater than 50 G because of imperfections in the vortex lattice. Considerations which we discuss in Sec. 4 suggest that a major imperfection such as a missing or extra vortex or dislocation or grain boundary would produce such a shift as far way as 1500 Å, so 80% of the sample must be more than 1500 Å from such a major imperfection. If we assume a polycrystalline model with large angle boundaries viewed as a sheet of such imperfections, the dimensions of the vortex crystallites must of order (1500 Å)$\times 2/0.2$, or more than ten lattice spacings at $B\cong\frac{1}{2}H_{c2}$. If we

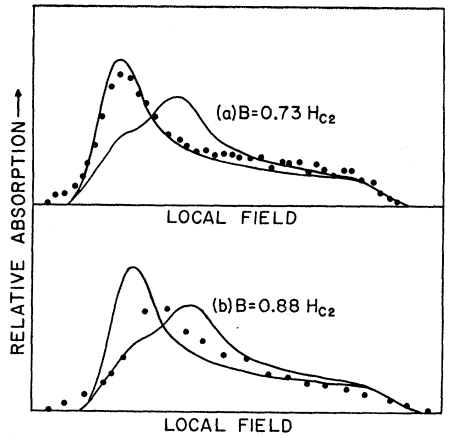

FIG. 3. Comparison between theoretical line shapes obtained by smearing the shapes of Fig. 2, with absorption line shape deduced from data of Fig. 1, as described in the text.

assume an otherwise perfect lattice with random vacancies, the vacancy concentration must be considerably less than $\frac{1}{10}$. If we assume, as is likely, that each vortex is randomly displaced from its equilibrium position as a result of impurity variations or other atomic lattice defects, the typical displacement is small, less than 10% of the lattice spacing, judging from Fig. 6 below, at intermediate fields. Our assumption used in making these estimates is fairly conservative.

III. MAGNETIZATION AND FLUX DENSITY

For a more detailed discussion of the line shape parameters it is of interest to know B and H as accurately as possible. For sample B, which was in the form of a stack of 0.1-mm foils with plastic tape and aluminum foil interspersed, B could be measured with at least ± 10 G precision down to 1000 G by increasing the field at the end of the field cycle in order to observe the aluminum nuclear resonance of nuclei inside the Al foil, instead of the vanadium resonance. Then exactly the same field cycling resonance (without the 100-Hz field) was done on the Al resonance. ν_p was varied until there was a sharp dip in the Al resonance, and the position of the dip gave the flux through the Al foils and thus through the vanadium also. As expected[17] for this geometry, the flux density B was nearly equal to the applied field H_e. Below $B \cong 1000$ G the aluminum resonance was too broad to observe, although it would probably be possible to see it by improving the aluminum-foil purity and thus, perhaps, the signal-to-noise ratio.

We also measured M to get $H \equiv B - 4\pi M$ and also to estimate B at low fields; our measurements agree well with those of Radebaugh and Keesom,[18] allowing for impurity differences. The same magnet and sample geometry (including interleaved tape and foil) were used but the NMR and miniature Dewar assembly was replaced with series opposed coils, coaxial with the superconducting magnet, and connected to a galvanometer and in later runs to a lock-in amplifier. The sample was reciprocated between the coils manually and later at 6 Hz (7-mm displacement) by a simple stirring motor-eccentric–connecting-rod combination. The apparatus was self-calibrated by turning the sample so that H_e was parallel to the sample surface, and measuring the slope of M versus H_e in the low-field Meissner region. Even though H_e is parallel to the foil surface, a demagnetization correction must be made: Between V foils, local $h = -4\pi M$, where M is the magnetization per unit of volume of the vanadium itself. Defining $\langle B \rangle$, $\langle M \rangle$ as averages over the entire sample volume including nonsuperconducting interleaving, we have $\langle B \rangle = (1-f)h = -(1-f)4\pi M$, where f is the fraction of the sample volume containing vanadium ($f \cong 0.3$ for this sample). The sample volume is more or less spherical, so $\langle B \rangle \cong H_e + \frac{2}{3}4\pi \langle M \rangle$; and $\langle M \rangle = fM$. Solving these equations we get $-4\pi M = H_e(1+f/3)$, in the low-field Meissner region, for the self-calibration runs.

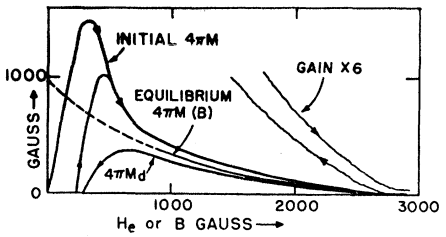

FIG. 4. Observed magnetization versus applied field, and inferred equilibrium magnetization versus flux density B.

The sample was then reoriented in the same way as was used in the NMR experiment with H_e perpendicular to the surface, and magnetization measured for upgoing and downgoing fields. Data for sample B at 1.4°K are shown in Fig. 4, together with an inferred M versus B curve. We verified that the apparent M was the same for a slow downgoing sweep as for a rapid field cycle, and could also observe the effect of the 100-Hz field. For values of 100-Hz field typically used in the NMR runs the difference between upgoing and downgoing magnetization curves was about one-half that without the 100-Hz field. This is the ac analog of the "jarring" effect noticed by Radebaugh and Keesom.

To estimate B at the lowest fields, we used the observed magnetization for downgoing H_e, which we denote by M_d. If the extra, hysteretic, magnetization is uniform (that is, resulting from edge currents around the sample) then $\langle B \rangle = B \cong H_e + \frac{2}{3}4\pi \langle M_d \rangle$ because the over-all sample volume is roughly spherical (it is in fact more nearly a cylinder whose length and diameter are equal). Since $\langle M_d \rangle = fM_d$, we have $B = H_e + 8\pi f M_d/3$. This small correction was roughly checked above 1000 G, where B, H_e, and M_d are all known.

To get the equilibrium-magnetization curve, the up and downgoing magnetization curves were averaged, for $H_e \gtrsim H_{c1}$. Then we replotted the average curve against B, using $B = H_e + 8\pi f M/3$, as above. Finally, at low fields where hysteresis was too great we extrapolated M versus B obtaining a fairly unique curve by the requirements that the area under the M versus B curve should equal $H_c^2/8\pi$; that $4\pi dM/dB$ be minus one in the limit $B \to 0$; and that the curve have negative d^2M/dB^2 and be reasonable looking. Essentially the same method was used by Keesom and Radebaugh. We assume that thermodynamic H_c is the same for our sample as theirs; it should not depend much on impurity content.

Similar measurements and corrections were made on sample A, which was in the form of 25 wires trans-

[17] J. Cape and J. M. Zimmerman, Phys. Rev. **153**, 416 (1967).
[18] P. R. Radebaugh and P. Keesom, Phys. Rev. **149**, 209 (1966); **149**, 217 (1966).

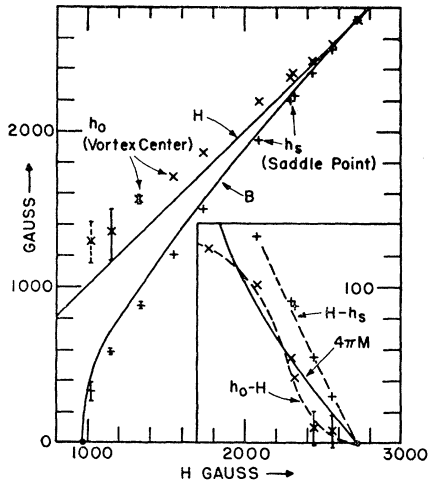

FIG. 5. Field at a vortex and at the saddle point, and also B, versus H. The inset shows the differences between H and the other fields on an expanded scale, near H_{c2}. All curves are purely experimental except B, which is slightly constrained by thermodynamics as described in the text. The same data were reported in Ref. 16, but H and B are slightly different because of improved magnetic measurements. The lowest h_0 data point was based on one run only, and is therefore shown dashed.

verse to H_e. Here we could not measure B directly, a serious disadvantage. For an infinite isolated cylinder,[17] $B=H_e+2\pi M$. For a randomly arranged bundle of wires, diameter small compared to the spacing between wires, this is also true because the field due to neighboring wires averages to zero. Correcting for finite length of the sample volume, which was roughly spherical as before, we conclude that $B\cong H_e+2\pi M+4\pi f M_d/6$.

For sample B, the flux density B is accurate to ± 10 G or better above 1000 G. All other field estimates may suffer from systematic errors due to the approximations outlined above. The error in B at low field, and in sample A, is probably less than $0.05(H-B)$. The error in $4\pi M=H-B$ is probably less than $0.1(H-B)$ at high field, conceivably more at low field. In sample A, the flux density B may be in error by about $0.05(H-B)$ for all runs.

The transition at H_{c2} was about 100 G wide in sample B, wider in sample A, but the average H_{c2} could be determined very accurately by extrapolating M versus H_e from above and below H_{c2}. For sample B, at 4.2°, $H_{c2}=850$ G, $H_{c1}\simeq 380$ G; at 1.41° $H_{c2}=2720$ G, and $H_{c1}\simeq 985$. For sample A, $H_{c2}=3420$ G at 1.33°K, and 3290 G at 1.5°K. The reader should consult the paper of Radebaugh and Keesom[18] for a thorough investigation of the magnetic and thermal parameters of pure vanadium.

IV. LOCAL FIELD MEASUREMENTS

The maximum field h_0 at the vortex center, and the saddle-point field h_s obtained from the absorption peak at the low-frequency end of the line, are plotted together with B, in Fig. 5, for sample B at 1.41°K. Other runs are summarized in Table I. We did not try to estimate the minimum field; it was always close to h_s as discussed in Sec. II.

We will compare our results with predictions based[10,14] on the Ginsburg-Landau equations, mostly in the limit appropriate only to dirty superconductors near H_{c2}. We do this, even though the theory should not apply to our samples,[19,20] because the theory is well defined and familiar. We assume a triangular lattice henceforth,[14] and denote the corresponding high-field solution to the Ginsburg-Landau equations by KRA.

Linewidth Versus Magnetization

The KRA solution predicts that[14,21] $(h_0-h_s)/4\pi M$ is 1.35. This ratio can be measured accurately in both samples A and B. It is significantly greater than the KRA value in the clean sample B, being around 2 for $B\simeq 1200$ G, and around 2.5 fairly close to H_{c2}. Very close to H_{c2} there is some indication that the ratio decreases again (see the next paragraph). In sample A the ratio is less, around 1.75 for most runs. This is the only difference we can discern between samples A and B. The data on sample A were too sketchy, and B in this sample too uncertain, to draw any other conclusions, and henceforth all analysis refers to the fairly clean sample B.

Field at a Vortex Center

In the KRA limit this field h_0 equals H. In sample B, h_0 is significantly greater than H. Marcus[20] has solved the Ginsburg-Landau equations in a cellular approximation for $\eta=2$, not too far from η_1 and η_2 for our sample. He predicts that h_0 should be greater than H but by only about half as much as we observe, over most of the range of B. The comparison is ambiguous since H_{c2}/H_{c1} is not quite the same for this calculation as for the sample.

TABLE I. Summary of line-shape runs not plotted in Figs. 5 and 6.

Sample	T°K	B	H	h_0	h_s
B	4.2	514	582	630	490
A	1.3	867	1235	1380	818
A	1.3	1915	2062	2150	1890
A	1.3	2625	2700	2740	2600
A	1.54	1180	1442	1560	1130
A	1.54	1925	2060	2155	1890
A	1.54	2635	2697	2730	2620

[19] For a review of relevant theoretical work see A. L. Fetter and P. C. Hohenberg, in A Treatise on Superconductivity, edited by R. D. Parks (Marcel Dekker, to be published).

[20] For theory applicable to clean material near T_c and H_{c2} see L. Neumann and L. Tewordt, Z. Physik 191, 73 (1966). This paper does not give an explicit field map.

[21] Lj. Dobrosavljevic, Compt. Rend. (to be published).

Near H_{c2} it appears that the curve for h_0 is becoming tangent to H. In other words, near H_{c2}, h_0-H may be proportional to $(H-H_c)^2$ (inset, Fig. 5). This is predicted by the Ginsburg-Landau equations, but as we mentioned they should not necessarily apply to pure vanadium. It is difficult for us to study this region accurately because H_{c2} evidently varies by about 3% over the sample volume, judging from the width of the transition in M at H_{c2}.

In the limit $B\to 0$, h_0 is the field at the center of an isolated vortex. We estimate it later as $(1.2\pm 0.2)H_{c1}$. In the high κ limit, the Ginsburg-Landau prediction is $h_0=2H_{c1}$; in the limit $\kappa=1/\sqrt{2}$, $h_0=H_{c1}$. Marcus,[22] and Neumann and Tewordt,[23] and Matricon[24] have solved the Ginsburg-Landau equations for an isolated vortex, for various κ values. They obtain the ratio of h_0 to H_{c1} as 1.07 for $\kappa=1$, 1.21 for $\kappa=2$, 1.35 for $\kappa=4$, and 1.39 for $\kappa=5$. Matricon[24] has also solved the problem with a two-quantum fluxoid and finds less than a 1% difference in this field ratio, between a single and a double flux quantum. Neumann and Tewordt[23] have estimated the correction to these results for a clean sample. The correction is large: For a sample having the same κ and mean free path as sample B, they predict that the center field will be around $1.4H_{c1}$, instead of $(1.2\pm 2)H_{c1}$ as observed, and around $1.07H_{c1}$ from the Ginsburg-Landau equations with $\kappa=1$. As usual, their theory is only valid near T_c.

Line Centroid

The flux density B is the center of gravity of the true field distribution, and is therefore expected to be close to the saddle-point singularity. For the Abrikosov limit,[21] $(h_s-B)/(h_0-h_s)$ is 0.26. In sample B this ratio is less, roughly 0.2 for $B\simeq\frac{1}{2}H_{c2}$, most probably because the line-shape function is relatively lower near h_0. The height of the line-shape function at h_0 is inversely proportional to $\partial^2 h/\partial r^2$ at the vortex center. So probably the field distribution is more sharply peaked at the vortex center than would be predicted by the KRA limit solution scaled up to the observed linewidth.

Field Distribution in Space

When the flux density is not too low ($B\gtrsim\frac{1}{2}H_{c2}$), the field variation in real space will not be too rapid and then the field can be mapped with an accuracy of a few percent from the four experimental line shape parameters B, h_0, h_s and the minimum field h_{min}. We expand $h(\mathbf{r})$ in a two-dimensional Fourier series, keeping the first ten terms: $h=\sum A_i \cos\mathbf{k}_i\cdot\mathbf{r}$. The k_i are vectors of the reciprocal lattice. The vector $k_0=0$ and $A_0=B$. We take $A_1=A_2=A_3$; $A_4=A_5=A_6$; $A_7=A_8=A_9$; $\mathbf{k}_1$, $\mathbf{k}_2$, $\mathbf{k}_3$ are equal, of magnitude $4\pi r_0/\sqrt{3}$, 120° apart in direction, and $\mathbf{k}_1$ is perpendicular to a primitive translation vector of the fluxoid lattice. The vectors $\mathbf{k}_7$, $\mathbf{k}_8$, $\mathbf{k}_9$ are, respectively, twice $\mathbf{k}_1$, $\mathbf{k}_2$, $\mathbf{k}_3$; and $\mathbf{k}_4$, $\mathbf{k}_5$, $\mathbf{k}_6$ are a similar trio of vectors of equal length 120° apart, with $\mathbf{k}_4=\mathbf{k}_1-\mathbf{k}_2$. Then calculation shows that $h_0=B+3(A_1+A_4+A_7)$; $h_s=B-A_1-A_4+3A_7$, $h_{\min}=B-1.5A_1+3A_4-1.5A_7$; and from these we get $A_1+A_4=\frac{1}{4}(h_0-h_s)$. From the data mentioned in the last paragraph we conclude that $A_7=(0.05\pm 0.05)A_1$, and if we take $h_s-h_{\min}$ as $(0.07\pm 0.05)(h_0-h_s)$ then we estimate that $A_4=(0.05\pm 0.05)A_1$. The errors stated here are only those from the conservative assumption of an error of 5% of the linewidth in the determination of h_0, h_s, and $h_{\min}$. They do not include errors resulting from the omission of higher-order Fourier components which are probably especially serious for A_7. Cribier *et al.*[11] conclude that, in niobium, A_4 and A_7 are small compared to A_1, but they set no limits on these components.

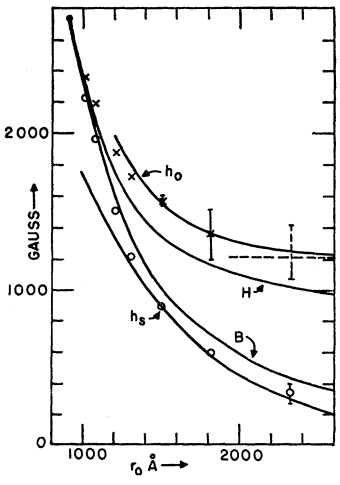

FIG. 6. Data of Fig. 5 replotted against vortex spacing, assuming the triangular lattice and the accepted fluxoid $hc/2e$. The curves passing through h_s and h_0 at large r_0 are based on the superposition model.

Low-Density Limit: Superposition Model

In the limit of very low B we would have an array of hardly interacting vortices. Call the field near such a vortex $h_i(r)$, where r is the distance from the center. It is interesting to interpret our data in terms of a model in which the field at any point is assumed to be the superposition of all fields due to (nearby) vortices, and these fields are assumed to be given by the same function $h_i(r)$ as for an isolated vortex.[25] In this model, since $h_i(r)$ falls off rapidly with r, we can include only near neighbors, and, if r_0 is the vortex lattice spacing,

[22] P. Marcus, in *Proceedings of the Ninth International Conference on Low-Temperature Physics, Columbus, Ohio*, 1964, edited by J. G. Daunt, D. O. Edwards, F. J. Milford, and M. Yaqub (Plenum Press, Inc., New York, 1965), p. 550.

[23] L. Neumann and L. Tewordt, Z. Physik **189**, 55 (1966).

[24] J. Matricon (private communication).

[25] Such a model has been considered at lower flux values by P. Marcus, in Proceedings of the Tenth International Conference on Low Temperature Physics, Moscow, 1966 (to be published).

the model predicts that $h_s=2h_i(r_0/2)$ and $h_0=h_i(0)+6h_i(r_0)$.

In Fig. 6, we replot the data of Fig. 5 versus $r_0=4.86\times10^{-4}B^{-1/2}$, the theoretical triangular lattice spacing. The lower curve, fitted to h_s, was obtained by assuming that $h_i(r)$ is proportional to $r^{-1/2}\exp(-r/\lambda_L)$, with $\lambda_L=400$ Å as estimated by Keesom and Radebaugh. This form for the field variation is predicted by the Ginsburg-Landau equations for high κ, or by the London equations. In practice, over the range of interest, this function is very well represented by $\exp(-r/380)$ times a constant. There is one adjustable parameter in this fitting (the constant multiplying vertical scale), not counting λ_L. In the region where the fit is good, the saddle point is 1.5 coherence lengths or more from the nearest vortex.

We then forced the prediction $h_0=h_i(0)+6h_i(r_0)$ through the measurement of h_0 at $r_0=1520$, by setting $h_i(0)=1210$ G and obtaining $h_i(r_0)$ from extrapolation of the form deduced in the previous paragraph without any change of scale of $h_i(r)$. In other words, we assume $h_0=h_i(0)+3h_s(2r_0)$, obtaining $h_s(2r_0)$ by exponential extrapolation of actual measurements and setting $h_i(0)=1210$ G. The two unprecise measurements for h_0 for the largest values of r_0 in Fig. 5 tend to corroborate this estimate; while an upper limit of 1400 G seems indicated by the requirement that $h_i(0)$ be appreciably less than the value of $h_0=1560$ G observed for $r_0=1520$ Å.

Carrying this model further, we can create a unique trial function for $h_i(r)$ for all r by assuming that $h_i(0)=1210$ G; that $h_i(r)$ decreases quadratically with r out to some transition radius beyond which it is proportional to $r^{-1/2}\exp(-r/\lambda_L)$; and that h_i is continuous and has a continuous first derivative at this radius. The transition radius needed to fit $h_i(0)$ and $h_i(r_0)$ as deduced from Fig. 6 is 650 Å. Interestingly, this is the same order of magnitude as the transition radius between spin diffusion and direct relaxation, as deduced in the immediately previous paper. The fluxoid predicted by this model is only about 12% greater than the accepted value. Sixty percent of this flux is within the 650 A radius. This field variation appears to agree well with that predicted by Neumann and Tewordt[23] near T_c.

The good agreement with the accepted fluxoid $hc/2e$ is not too surprising since, given h_0 and h_s and the correct lattice, any smooth trial distribution is likely to give nearly the correct flux density and thus fluxoid provided the actual distribution is fairly smooth, as it is for $r_0=1510$ Å. Likewise, lengths of the order of 500 Å and fields of the order of 1000 G are built into the model. Also, the curve for h_s becomes significantly modified if more than nearest vortices are taken into account; it is about 30% higher at 1520 Å but only about 10% higher at 2300 Å. Good agreement would be obtained by increasing λ_L by perhaps 10% to about 500 Å, and the field at an isolated vortex center to about 1250 G. Such a detailed, three-parameter analysis does not seem worth while; the main point is to get a reasonable estimate of $h_i(0)$ and of the effect of vortex-lattice imperfections, which we used in Sec. II, and to show that the superposition model is not grossly wrong.

In conclusion we should mention that this does not constitute a direct measure of the penetration depth except insofar as the fluxoid is known and the model is correct. If the fluxoid were increased by a factor of 2, agreement would still be as good if we increased all lengths by the square root of 2.

V. MISCELLANEOUS EFFECTS

At the end of the introduction to this paper we mentioned that there appears to be an enhancement of the probe field intensity as the external field is lowered below H_{c2}, and we conjectured that this enhancement was due to the production of a large probe-frequency field in the H_e direction, which produces transitions by virtue of a residual quadrupole interaction. We have some independent evidence for this mechanism; At low H_e, around 1000 G, and higher probe power, absorption appeared at a frequency range double that of the main absorption presumably due to $\Delta m_I=\pm2$ transitions. We did not study this effect in detail, though it would be interesting to do so; mostly it was a nuisance which introduced uncertainty into the measurements at low B. At higher B this line disappeared rapidly, presumably because of a decreased admixture of states and also a decrease in the available probe power.

Near H_{c2}, where we usually did not use the 100-Hz field along H_e, we observed partial motional narrowing of the line when we applied a strong 100-Hz field. The dip in subsequent signal at h_s started to disappear and a new dip appeared at a frequency $\gamma B/2\pi$, where B is the independently measured average field.

ACKNOWLEDGMENTS

I would like to thank P. Marcus and G. Lasher for many useful conversations; L. Matricon, D. St. James, and B. Jacrot for sending me unpublished work; B. Silbernagel, A. Seeger, and A. Gossard for comments; and all the workers mentioned in the previous article for experimental help. W. Fite built much of the apparatus.